J. Fluid Mech. (1987), *vol.* 174, *pp.* 327–356
Printed in Great Britain

A plate oscillating across a liquid interface: effects of contact-angle hysteresis

By G. W. YOUNG
Department of Mathematics, University of Akron, Akron, OH 44325, USA

AND S. H. DAVIS
Department of Engineering Sciences and Applied Mathematics, Northwestern University, Evanston, IL 60201, USA

(Received 7 October 1985 and in revised form 27 May 1986)

We consider the oscillatory motion of a solid plate into and out of a bath of liquid. Assuming that the displacement amplitude of the plate motion is small and that the capillary number is small, the problem reduces to solving an interfacial boundary-value problem for the response of the contact line. The characteristic contact angle versus contact-line speed relationship includes contact-angle hysteresis which is assumed small and comparable to the amplitude of the plate motion. Sinusoidal and square-wave plate motions are considered. We find that the contact line moves with the plate if the contact line is fixed, but has relative motion otherwise. It would then advance part of the time, recede part of the time, and remain stationary in the transition periods. Further, we find that both contact-angle hysteresis and steepening of the contact angle with increasing contact-line speed are dissipative effects.

1. Introduction

The motion of a contact line formed by, say, a liquid, a gas and a solid is affected by its wetting and mobility properties. These enter a continuum description of the dynamics through a relationship between the contact angle θ and the speed U_{CL} of the contact line. This relationship

$$\theta = G(U_{CL}), \tag{1.1}$$

if measured in the laboratory, has the form shown in figure 1 in which θ increases with U_{CL} but has a jump at $U_{CL} = 0$. It can be argued (Dussan V. 1979) that a relation such as (1.1) should also hold for the actual angle θ as well. In this case the existence of the interval $\phi_A - \phi_R$ at zero speed is called contact-angle hysteresis where ϕ_A and ϕ_R are the advancing (liquid displaces gas) and receding (gas displaces liquid) static angles respectively. The contact line can advance only if $\theta > \phi_A$, and can recede only if $\theta < \phi_R$. The contact line is stationary for $\phi_R \leqslant \theta \leqslant \phi_A$. Such issues are discussed in detail by Dussan V. (1979).

The presence of contact-angle hysteresis can lead to finite-length portions of a contact line remaining stationary. Dussan V. & Chow (1983) and Dussan V. (1985) consider how a liquid drop on a tilted plate readjusts its contact line in order to progress down the plate. The front of the drop must advance while the rear must recede. They find in the presence of contact-angle hysteresis that a straight-line fixed portion must exist on each side of the drop along which $U_{CL} = 0$ and θ changes continuously from ϕ_R to ϕ_A.

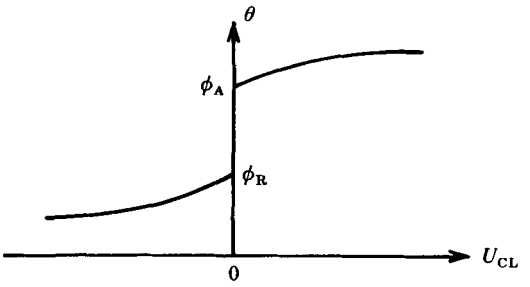

FIGURE 1. Sketch of experimental results of contact angle θ versus contact-line speed U_{CL}. $U_{CL} > 0$ denotes liquid displacing gas; $U_{CL} < 0$ denotes gas displacing liquid.

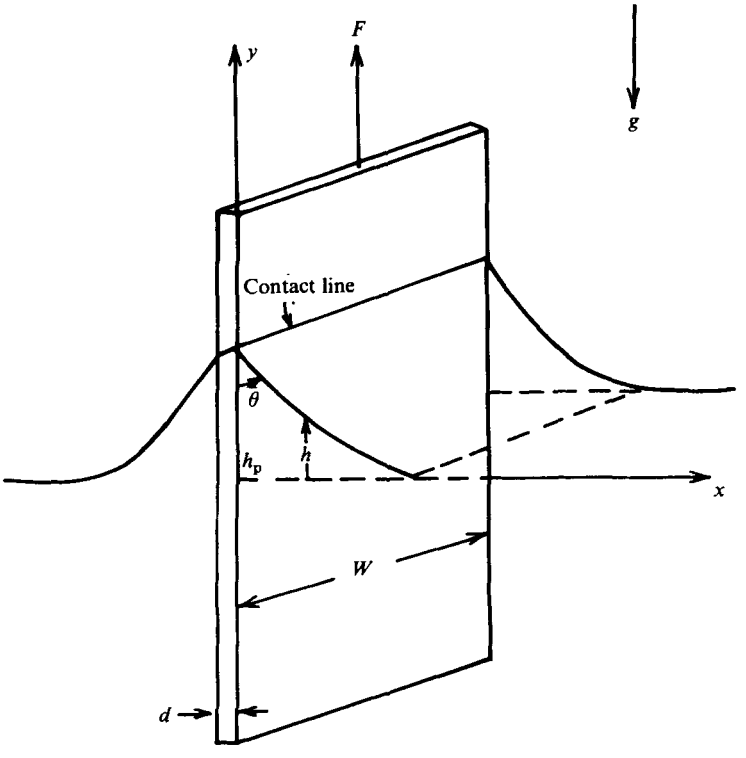

FIGURE 2. Sketch of a plate being moved into and out of a bath of fluid. The interfacial height h is measured relative to the flat interface far from the contact line. h_p is a reference point on the plate.

In the present work we address an analogous property of systems that possess contact-angle hysteresis. A contact line that reverses the direction of its motion must remain stationary for a non-zero time interval. We consider a plate that oscillates into and out of a bath of liquid as shown in figure 2. Wilhelmy-plate experiments leading to the measurement of dynamic contact-angle characteristics are based upon such an apparatus. During a complete cycle of the plate oscillation, the contact line undergoes both an advancing and a receding motion. The concern of this work is the transition behaviour between these two types of motions.

The Wilhelmy-plate apparatus or wetting-balance technique has been used to investigate contact-angle behaviour. Here the force F required to immerse/withdraw

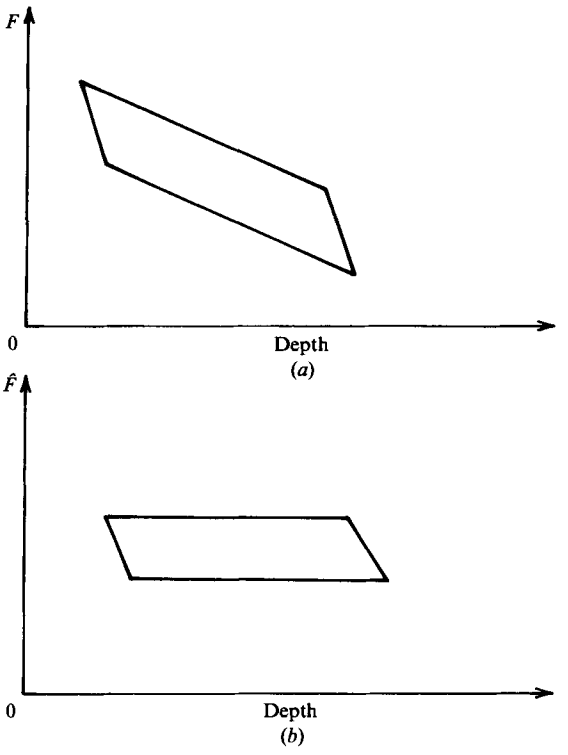

FIGURE 3. Immersion curves from Guastalla (1957, figure 11) of force on the moving Wilhelmy plate as a function of its depth of immersion, (*a*) uncorrected for buoyancy and (*b*) corrected for buoyancy.

the plate is measured and the contact angle is then calculated from the following expression derived from a static force balance:

$$\cos\theta = \left(\frac{1}{P\sigma}\right)(F+\rho gHWd), \tag{1.2}$$

where P, W, d and H are, respectively, the perimeter, width, thickness and depth of immersion of the plate which experiences a force F. Here g is the acceleration due to gravity, σ is the surface tension of the interface and ρ is the density of the liquid. Experiments are run at constant plate velocities within the range 0.1 mm/min–250 mm/min.

Johnson, Dettre & Brandreth (1977) immerse microscope slides coated with four different substrates into baths of water or hexadecane. They find that for certain fluid/fluid/solid systems the contact angle changes with the speed of the contact line, while for other systems the effect of contact-line speed on the contact angle appears to be negligible. In those cases where speed does affect the contact angle, they report an increase in contact angle for advancing motions and a decrease in contact angle for receding motions. In addition, they find that the variation of the contact angle with the contact-line speed could be quite different depending upon whether the motion is advancing or receding.

Penn & Miller (1980*a*, *b*) run experiments only at very small frequencies ω (20 min period, or longer) and find that under these conditions the contact angles remain constant for all fluid/fluid/solid systems considered. They report that the angle changes only during the conversion from advancing to receding motions, or vice

versa. At this time they observe that the contact line is stationary with respect to the plate.

Data collected using the Wilhelmy-plate apparatus is normally reported in the form of a graph of force versus depth of immersion. Guastalla (1957) reports immersion curves like those shown in figure 3. From these he calculates the 'work of dewetting' for the system. Johnson & Dettre (1969) suggest that the openness of the immersion curves, as reported by Guastalla and others, indicates the presence of contact-angle hysteresis.

To examine this hypothesis and further explore the effects of the presence of contact-angle hysteresis, we develop a system of equations governing the motion of the contact line induced by the oscillating plate. Sinusoidal and square-wave (Murphy 1984) plate motions are considered. The former type has continuous forcing and allows us to probe the contact-line response as a function of the relevant parameters. The latter type of motion most closely approximates the experimental set-ups in which the plate is moved at constant speed.

2. Formulation

Consider a plate moving vertically into and out of an infinite bath of liquid as shown in figure 2. We set up a coordinate system along and perpendicular to the plate such that the height of the fluid interface is zero as $x \to \infty$. In addition we assume that the problem is two-dimensional so that the contact line is a straight line normal to the (x, y)-plane.

The position of the plate at $x = 0$ and any time t is described by

$$h_{\mathrm{p}} = D \sin \omega t, \tag{2.1}$$

where h_{p} is a material point on the plate, $2D$ is the amplitude of the plate motion, and ω is its angular frequency of oscillation so that speed of the plate is

$$V_{\mathrm{p}} = D\omega \cos \omega t. \tag{2.2}$$

The liquid flow is governed by the Navier–Stokes and continuity equations. The gas is considered passive in that its viscosity and density are negligible. The boundary conditions on the liquid–gas interface at $y = h(x, t)$ are the kinematic, the normal stress balancing the (constant) surface tension σ times the curvature and the shear stress vanishing. Since the contact line may move, the imposition of the no-slip condition on the plate leads to a force singularity (Dussan V. & Davis 1974). Some means, such as the posing of effective slip, must be used to remove the singularity. Also, no liquid penetrates the solid. The remaining conditions required are those at the contact line. There is the condition of contact,

$$h(0, t) = A(t), \tag{2.3}$$

where $y = A(t)$ locates the contact line. In posing the condition of contact angle versus speed of the contact line, we allow hysteresis but simplify the variation by posing a piecewise-linear model as shown in figure 4; we have

$$\left.\begin{aligned} \theta &= \phi_{\mathrm{A}} + G'(0^+)\, U_{\mathrm{CL}}, & U_{\mathrm{CL}} &> 0 \\ \theta &= \phi_{\mathrm{R}} + G'(0^-)\, U_{\mathrm{CL}}, & U_{\mathrm{CL}} &< 0 \\ \phi_{\mathrm{R}} &\leqslant \theta \leqslant \phi_{\mathrm{A}}, & U_{\mathrm{CL}} &= 0 \end{aligned}\right\} \quad \text{at } x = 0, \quad y = A(t), \tag{2.4}$$

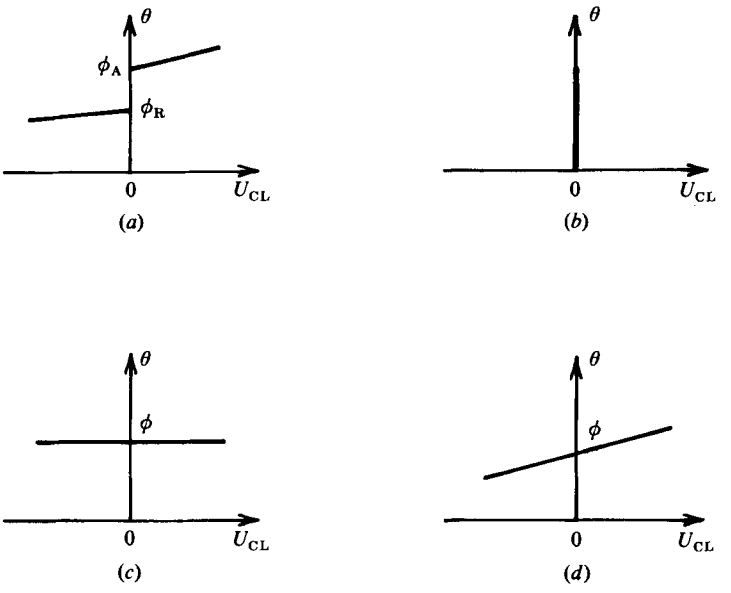

FIGURE 4. Sketch of possible relationships between the contact angle θ and the contact speed U_{CL}; (*a*) contact-angle hysteresis; (*b*) fixed contact line; (*c*) fixed contact angle; (*d*) smooth contact-angle variation.

where
$$\theta = \tan^{-1}(h_x) + \tfrac{1}{2}\pi. \tag{2.5}$$

We scale the governing system as follows:

$$x \to L_c = \left(\frac{\sigma}{\rho g}\right)^{\frac{1}{2}}, \tag{2.6a}$$

$$y \to L_c, \tag{2.6b}$$

$$t \to \omega^{-1}, \tag{2.6c}$$

$$\text{speed} \to \omega D, \tag{2.6d}$$

$$\text{pressure} \to \frac{\mu\omega D}{L_c}, \tag{2.6e}$$

$$h \to D. \tag{2.6f}$$

where μ is the viscosity; and $\nu = \mu/\rho$. Here L_c, the capillary lengthscale, is appropriate for static menisci and the pressure scale is consistent with slow viscous flow. These scalings give rise to the following non-dimensional groups:

$$\alpha = \frac{D}{L_c} = \left(\frac{\rho g D^2}{\sigma}\right)^{\frac{1}{2}}, \tag{2.7a}$$

$$C = \frac{\mu L_c \omega}{\sigma} = \left(\frac{\mu^2\omega^2}{\rho g \sigma}\right)^{\frac{1}{2}}, \tag{2.7b}$$

$$B = \frac{\rho g \delta_s^2}{\sigma} = \frac{\delta_s^2}{L_c^2} = \frac{g\mu}{\omega\sigma}, \tag{2.7c}$$

	Water		Ethyl alcohol		Glycerine	
	$\rho = 1.0$ gm/cm^3		$\rho = 0.79$ gm/cm^3		$\rho = 1.26$ gm/cm^3	
	$\nu = 1.14 \times 10^{-2}$ cm^2/s		$\nu = 1.70 \times 10^{-2}$ cm^2/s		$\nu = 18.5$ cm^2/s	
	$\sigma = 72.8$ dyn/cm		$\sigma = 22.0$ dyn/cm		$\sigma = 63.0$ dyn/cm	
ω (rad/s)	C	B	C	B	C	B
5×10^{-3}	2.11×10^{-7}	31.3	5.09×10^{-7}	122.0	4.14×10^{-4}	7.40×10^{4}
1×10^{-2}	4.23×10^{-7}	15.6	1.02×10^{-6}	61.0	8.27×10^{-4}	3.70×10^{4}
5×10^{-2}	2.11×10^{-6}	3.13	5.09×10^{-6}	12.2	4.14×10^{-3}	7.40×10^{4}
1×10^{-1}	4.23×10^{-6}	1.56	1.02×10^{-5}	6.10	8.27×10^{-3}	3.70×10^{3}
5×10^{-1}	2.11×10^{-5}	3.13×10^{-1}	5.09×10^{-5}	1.22	4.14×10^{-2}	7.40×10^{2}
1	4.23×10^{-5}	1.56×10^{-1}	1.02×10^{-4}	6.10×10^{-1}	8.27×10^{-2}	3.70×10^{2}
5	2.11×10^{-4}	3.13×10^{-1}	5.09×10^{-4}	1.22×10^{-1}	4.14×10^{-1}	7.40×10
10	4.23×10^{-4}	1.56×10^{-2}	1.02×10^{-3}	6.10×10^{-2}	8.27×10^{-1}	3.70×10
100	4.23×10^{-3}	1.56×10^{-3}	1.02×10^{-2}	6.10×10^{-3}	8.27	3.70
1000	4.23×10^{-2}	1.56×10^{-4}	1.02×10^{-1}	6.10×10^{-4}	8.27×10	3.70×10^{-1}

TABLE 1. For various values of the angular frequency of plate oscillation ω the capillary number C $(\rho\nu^2\omega^2/g\sigma)^{\frac{1}{2}}$, and Bond number $B = (g\rho\nu/\sigma\omega)$ are tabulated for the three fluids: water, ethyl alcohol and glycerine. Note that C is small for a wide range of ω

where α is a ratio of the maximum plate immersion to the capillary lengthscale, C is the capillary number, and B is a Bond number based upon the Stokes lengthscale

$$\delta_S = \left(\frac{\nu}{\omega}\right)^{\frac{1}{2}}. \tag{2.8}$$

B^{-1} plays the role of the Reynolds number in the present system. Further, there is a non-dimensional number that measures the effective slip or its equivalent.

We shall be examining the limit

$$\alpha = \left(\frac{\rho g D^2}{\sigma}\right)^{\frac{1}{2}} \ll 1, \tag{2.9}$$

which can be realized for Wilhelmy-plate experiments by immersing the plate only a small depth $2D$ into the liquid.

We now consider the size of the capillary number C and Bond number B. In table 1 we list values of these parameters for water, ethyl alcohol and glycerine as the frequency ω varies from 5×10^{-3} to 10^3. These values of ω correspond to oscillation periods ranging from 21 min to 6×10^{-3} s. Table 1 clearly shows that for the lower viscosity liquids, C is always extremely small. The same holds true for the more viscous oil as long as $\omega < 1$ rad/s. Thus we shall also assume that

$$C \ll 1. \tag{2.10}$$

At this time we make no assumptions on the order of B since its value changes more widely as ω varies. Further, the 'slip coefficient' is presumed fixed.

We shall assume that the advancing angle ϕ_A is near $\frac{1}{2}\pi$,

$$\phi_A = \tfrac{1}{2}\pi + \gamma\alpha, \tag{2.11}$$

and that the hysteresis, though non-zero, is small,

$$\phi_A - \phi_R = M\alpha. \tag{2.12}$$

Here γ and M are order-unity constants for $\alpha \to 0$. If $\gamma > 0$ then, $\phi_A > \frac{1}{2}\pi$ while if $\gamma < 0$, then $\phi_A < \frac{1}{2}\pi$. If $M = 0$, then hysteresis is absent.

We fix the slip, first take the limit $\alpha \to 0$ and then the limit $C \to 0$, with $B = O(1)$, to obtain the interfacial boundary-value problem

$$h_{0xx} - h_0 = 0 \tag{2.13}$$

subject to the contact-line boundary condition at $x = 0$,

$$\left.\begin{aligned} \dot{A}_0 - \cos t = V_A[h_{0x} - \gamma], \quad & \dot{A}_0 - \cos t > 0 \\ \dot{A}_0 - \cos t = V_R[h_{0x} - \gamma + M], \quad & \dot{A}_0 - \cos t < 0 \\ \gamma - M \leqslant h_{0x} \leqslant \gamma, \quad & \dot{A}_0 - \cos t = 0 \end{aligned}\right\}. \tag{2.14}$$

Here t is the scaled time, a dot denotes $\mathrm{d}/\mathrm{d}t$ and subscripts x denote partial differentiation. In conditions (2.14)

$$V_A = \frac{1}{\omega G'(0^+) L_c}, \tag{2.15a}$$

$$V_R = \frac{1}{\omega G'(0^-) L_c}. \tag{2.15b}$$

Since $G'(0^+)$ has units of inverse velocity, then V_A characterizes the ratio of the actual contact-line speed to the laboratory contact-line speed. V_R has an analogous interpretation. We note here that fixed contact angles have the $G'(0) = 0$ so that $V_A \to \infty$ and $V_R \to \infty$. However, these approach infinity also if $\omega \to 0$. Thus, systems cycled with small ω may *appear* to exhibit fixed contact angles even though the $G'(0) \neq 0$. Further, if the $G'(0) \to \infty$ so that $V_A \to 0$ and $V_R \to 0$, then the contact line is fixed to the plate. Such behaviour may appear to hold if $\omega \to \infty$.

Equation (2.13) balances surface tension and hydrostatic forces while (2.14) gives the contact-angle condition including hysteresis. This problem decouples (Young 1985) from the flow problem which can be solved given the solution for the leading-order interface shape h_0 and leading-order contact-line position A_0. In particular the problem for h_0 is independent of the slip model posed and would be independent of whatever device is used to remove the contact-line singularity present when the no-slip condition is enforced. The range of validity of this solution *would*, of course, depend on the 'amount of slip'. For example, if the slip were small, then the velocity gradients would be large near the contact line and one would have to make C exceedingly small in order to decouple the flow field from the interfacial problem posed above.

3. Force balance

The solution to system (2.13) and (2.14) can be used to obtain approximate formulae for the force balance on a finite plate oscillating through a liquid–gas interface. Let us consider a plate of height $2l$, $D \leqslant l$, width W and thickness d, suspended in a bath of liquid of viscosity μ and density ρ as shown in figure 2. Let the motion of a point on the centre of the plate be described by (2.1) so that the depth of immersion H of the plate into the liquid is given by

$$H = D(1 - \sin \omega t) + (l - D) = l - D \sin \omega t. \tag{3.1}$$

Here we assume that the plate is at the top of its stroke at time $t = \pi/2\omega$ and that a portion of the plate of length $l-D$ is still submerged. A dynamic balance of the forces acting on the plate requires that

$$M_s \frac{dV_p}{dt} = -M_s g + F + \rho g H W d - 2(d+W)\sigma\cos\theta + 2\mu\int_A \frac{\partial v}{\partial x}\,dA, \tag{3.2}$$

where $M_s = 2\rho_s l W d$ is the mass of the plate whose density is ρ_s. The right-hand side of (3.2) represents the gravitational, suspension, buoyant, surface tension and drag forces on the plate respectively. Note that for a thin plate, small d, we can neglect the drag forces on the thin edges and then A represents the areas of the flat faces.

If all the force terms are known, then measuring F determines the contact angle θ. For θ given by (2.5) the scaled force balance for small d becomes

$$\cos\theta = -h_x(1+\alpha^2 h_x^2)^{-\frac{1}{2}} = \frac{F}{2W\sigma\alpha} - \frac{M_s g}{2W\sigma\alpha} + \frac{d}{2L_c}\left(\frac{l}{D} - \sin t\right) + \frac{M_s D\omega^2}{2W\sigma\alpha}\sin t + C\int_A \frac{\partial v}{\partial x}\,dy\,dz, \tag{3.3}$$

where z, the spanwise spatial coordinate, is scaled on W.

Under the small-d, small-α, and small-C assumptions, we neglect the drag forces on the plate so that (3.3) becomes

$$-h_{0x} = \hat{F}, \quad x = 0, \tag{3.4a}$$

where

$$\hat{F} = \frac{1}{2W\sigma\alpha}\left\{F - M_s g + DWd\rho g\left(\frac{l}{D} - \sin t\right) + M_s D\omega^2 \sin t\right\}. \tag{3.4b}$$

$\hat{F}$ measures the suspension force, gravitational force, buoyant force and a contribution due to the acceleration of the plate.

The neglect of the drag force can be justified by finding the solution to the leading-order flow field and evaluating the last term of (3.3). Since the velocity field would depend on the effective slip coefficient, the neglect of the drag would be justified *a posteriori* if C is small enough. The criterion for 'small enough' would depend on the slip; the smaller the slip the smaller that C must be.

One can post an *a priori* though a much stricter limitation on C for the neglect of the drag. When d, α and C are small, the smallest contributions to (3.3) are the buoyant and drag forces. We neglect the latter compared with the former if $C \ll d/L_c$ which implies that $\nu\omega g^{-1} d^{-1} \ll 1$. This is satisfied for $\omega \leqslant 1$ rad/s and $d \geqslant 0.02$ cm for the fluids tested in table 1.

4. Solutions

The solution of (2.13) is

$$h_0 = C(t)\exp(-x), \tag{4.1}$$

where $C(t)$ is an unknown function of time determined by the contact-line boundary condition (2.14). Since the motion of the plate is periodic, we expect that the interfacial response will also be periodic after all initial transients have decayed. We seek such a periodic solution. Let us begin then at time $t = \frac{1}{2}\pi$ when the plate is at the top position of the cycle according to the scaled version

$$h_p = \sin t \tag{4.2}$$

of (2.1). At this point we assume that the contact-line speed is given by

$$\dot{A}_0 - \cos t = -S < 0 \tag{4.3}$$

since the plate is being withdrawn from the bath just prior to $t = \frac{1}{2}\pi$. Thus, the contact line is receding. From the periodicity assumption, S must be chosen so that (4.3) also holds at $t = \frac{5}{2}\pi$; S will, of course, depend on V_A, V_R, γ and M. Assuming that we have such an S, we can now solve for $C(t)$.

Equation (4.3) requires us to use the receding portion of (2.14):

$$\dot{A}_0 - \cos t = V_R[h_{0x} - \gamma + M]. \tag{4.4}$$

We substitute for A_0 using (2.3) and (4.1) into (4.4) and find that

$$\dot{C} + V_R C = \cos t + V_R[-\gamma + M], \tag{4.5}$$

the solution of which gives

$$C(t) = C_0^- \exp(-V_R t) + (M - \gamma) + \frac{V_R \cos t + \sin t}{V_R^2 + 1}. \tag{4.6}$$

In this expression C_0^- is a constant of integration.

The constant C_0^- is obtained by satisfying (4.3). We find that

$$C_0^- = \left[S - \frac{V_R}{V_R^2 + 1}\right] \frac{\exp(\frac{1}{2}\pi V_R)}{V_R}. \tag{4.7}$$

Therefore, h_0 is given by

$$h_0 = \exp(-x)\left\{C_0^- \exp(-V_R t) + [M - \gamma] + \frac{V_R \cos t + \sin t}{V_R^2 + 1}\right\}. \tag{4.8}$$

However, this is only valid when the contact-line speed is negative. At time $t = \frac{3}{2}\pi$, the plate is being pushed into the bath. Therefore, the contact line will want to advance so the contact-line speed must undergo a transition from a receding to an advancing motion. Its speed must pass through zero in order to do this. We assume that (4.8) is valid up until a time t_1 where

$$\dot{A}_0 - \cos t_1 = 0. \tag{4.9}$$

According to (4.4), this implies that the contact angle at t_1 is

$$h_{0x} = \gamma - M, \tag{4.10}$$

which is the receding angle ϕ_R. If we substitute (4.8) into (4.9), we find that t_1 satisfies

$$V_R\left[C_0^- \exp(-V_R t_1) + \frac{V_R \cos t_1 + \sin t_1}{V_R^2 + 1}\right] = 0. \tag{4.11}$$

We find the solution t_1 numerically by using Newton's method. Up to this point (4.8) is valid for $\frac{1}{2}\pi \leqslant t \leqslant t_1$. We note here that we require $t_1 < \frac{3}{2}\pi$ and find this to be true for all parameter values tested.

From (2.14) we see that since we are at contact angle ϕ_R at $t = t_1$, the contact line must remain fixed until the angle changes to ϕ_A. Only then can the contact line advance as the plate is pushed in. So we use the fixed portion of (2.14) and substitute (4.1) into

$$\dot{A}_0 - \cos t = 0. \tag{4.12}$$

We find that

$$C(t) = C_0^0 + \sin t, \tag{4.13}$$

where C_0^0 is a constant of integration found by satisfying (4.10) at $t = t_1$, viz.

$$C_0^0 = M - \gamma - \sin t_1. \tag{4.14}$$

Thus, h_0 is given by

$$h_0 = \exp(-x)\{\sin t - \sin t_1 + M - \gamma\}. \tag{4.15}$$

This expression is valid until the time $t = t_2$ when the contact angle reaches ϕ_A,

$$h_{0x} - \gamma = 0. \tag{4.16}$$

We substitute (4.15) into (4.16) and find that

$$t_2 = \sin^{-1}[\sin t_1 - M]. \tag{4.17}$$

This expression is consistent with $\frac{1}{2}\pi < t_1 < t_2 < \frac{3}{2}\pi$ since the sine decreases for this range. Therefore the contact line remains fixed for times $t_1 \leqslant t \leqslant t_2$, during which the expression (4.15) is valid. We note that the interval of time $t_2 - t_1$ that the contact line is fixed increases as M increases. This is consistent with (2.12) since increasing M implies the increasing of the contact-angle hysteresis. In addition, t_2 also depends upon the plate motion through $\sin t_1$.

At $t = t_2$, we are at the advancing contact angle ϕ_A. The plate is still being pushed in, so the contact line wants to advance. Conditions (2.14) require us to use the advancing portion

$$\dot{A}_0 - \cos t = V_A[h_{0x} - \gamma]. \tag{4.18}$$

If we substitute (4.1) into (4.18), we obtain

$$\dot{C} + V_A C = \cos t - V_A \gamma, \tag{4.19}$$

the solution of which gives

$$C(t) = C_0^+ \exp(-V_A t) - \gamma + \frac{V_A \cos t + \sin t}{V_A^2 + 1}. \tag{4.20}$$

In this expression C_0^+ is a constant of integration obtained through the matching of (4.1) with (4.15) at time $t = t_2$. We find that

$$C_0^+ = -\left[\frac{V_A \cos t_2 + \sin t_2}{V_A^2 + 1}\right] \exp(V_A t_2) \tag{4.21}$$

and thus h_0 is given by

$$h_0 = \exp(-x)\left\{C_0^+ \exp(-V_A t) - \gamma + \frac{V_A \cos t + \sin t}{V_A^2 + 1}\right\}. \tag{4.22}$$

This expression is valid as long as the contact line is advancing. However, eventually the plate is withdrawn from the bath for $\frac{3}{2}\pi \leqslant t \leqslant \frac{5}{2}\pi$, and thus the contact line will want to recede. The contact line changes from an advancing to a receding motion during which time its speed passes through zero. Therefore, (4.22) is valid until the time t_3 where

$$\dot{A}_0 - \cos t_3 = 0. \tag{4.23}$$

From (4.18) we have that the contact angle at t_3 is

$$h_{0x} - \gamma = 0, \tag{4.24}$$

which is the advancing angle ϕ_A. If we substitute (4.22) into (4.23), we find that t_3 satisfies

$$V_A\left[C_0^+ \exp(-V_A t_3) + \frac{V_A \cos t_3 + \sin t_3}{V_A^2 + 1}\right] = 0. \tag{4.25}$$

We find the solution t_3 numerically using Newton's method. So (4.22) is valid for $t_2 \leqslant t \leqslant t_3$.

Similarly to before, the contact line will remain fixed until the contact angle

changes to ϕ_R. Then it will begin to recede. We find that the contact line remains fixed until

$$t_4 = \sin^{-1}[\sin t_3 + M] \tag{4.26}$$

and during this time

$$h_0 = \exp(-x)\{\sin t - \sin t_3 - \gamma\}. \tag{4.27}$$

We note that for all cases tested we find that $\frac{3}{2}\pi < t_3 < t_4 < \frac{5}{2}\pi$ so the plate has not reached the top of the cycle at t_4. Thus, it is still being pulled up and the contact line is receding. Again (4.4) applies and we have

$$h_0 = \exp(-x)\left\{C_0^* \exp(-V_R t) + [M-\gamma] + \frac{V_R \cos t + \sin t}{V_R^2 + 1}\right\}, \tag{4.28}$$

where C_0^* is chosen so that (4.28) matches (4.27) at t_4. We find

$$C_0^* = -\left[\frac{V_R \cos t_4 + \sin t_4}{V_R^2 + 1}\right] \exp(V_R t_4). \tag{4.29}$$

Now in order to satisfy the periodicity requirement, we need (4.8) evaluated at $t = \frac{1}{2}\pi$ to match (4.28) evaluated at $t = \frac{5}{2}\pi$. This condition reduces to

$$C_0^- \exp(-\tfrac{1}{2}\pi V_R) = C_0^* \exp(-\tfrac{5}{2}\pi V_R). \tag{4.30}$$

This expression is satisfied by the correct choice of the initial speed S. We determine S by the following iterative procedure. We assign the initial value $S = 1$ and solve to obtain (4.28). We then calculate the contact-line speed at $t = \frac{5}{2}\pi$. We use this value as the next guess for S and repeat the procedure until successive iterates agree to within 0.1 %.

In summary, we have that h_0 is given by the following regimes as shown in table 2:

(i) $\frac{1}{2}\pi \leqslant t \leqslant t_1$, (4.8) holds and the contact line recedes;
(ii) $t_1 \leqslant t \leqslant t_2$, (4.15) holds and the contact line is fixed;
(iii) $t_2 \leqslant t \leqslant t_3$, (4.22) holds and the contact line advances;
(iv) $t_3 \leqslant t \leqslant t_4$, (4.27) holds and the contact line is fixed;
(v) $t_4 \leqslant t \leqslant \frac{5}{2}\pi$, (4.28) holds and the contact line recedes, matching with (4.8) at the top of the cycle.

5. Results and discussion

One extreme case of contact-line behaviour is that of fixed contact lines. Here $G'(0^+) = G'(0^-) = \infty$ so that $V_A = V_R = 0$. Thus,

$$\dot{A}_0 - \cos t = 0 \tag{5.1}$$

for all time. This is consistent with the V_A, $V_R \to 0$ limits of forms (4.8), (4.22) and (4.28), viz.

$$h_0 = \exp(-x)\{k_0 + \sin t\}, \tag{5.2}$$

where k_0 is a constant. The solution (5.2) satisfies (5.1) and the fixed-line portions of (4.15) and (4.27).

A second extreme case of contact-line behaviour is that of fixed contact angles. Here $G'(0^+) = G'(0^-) = 0$ so that $V_A = V_R = \infty$, and the laboratory contact-line speed is zero. Thus, the contact angle is either ϕ_A or ϕ_R and the actual contact-line speed is equal and opposite to the plate speed. Therefore,

$$\dot{A}_0 - \cos t = -\cos t \tag{5.3}$$

$t_0 = \frac{1}{2}\pi$	Top of the plate stroke	Receding
t_1	Contact angle = ϕ_R	Fixed
t_2	Contact angle = ϕ_A	Advancing
$t = \frac{3}{2}$	Bottom of the plate stroke	Advancing
t_3	Contact angle = ϕ_A	Fixed
t_4	Contact angle = ϕ_R	Receding
$t^* = \frac{5}{2}$	Top of the plate stroke	

(*a*)

$t_0 = t_1 = \frac{1}{2}\pi$	Top of the plate stroke contact angle = ϕ_R	Fixed
t_2	Contact angle = ϕ_A	Advancing
$t_3 = \frac{3}{2}\pi$	Bottom of the plate stroke contact angle = ϕ_A	Fixed
t_4	Contact angle = ϕ_R	Receding
$t^* = \frac{5}{2}$	Top of the plate stroke	

(*b*)

TABLE 2. Schematic of the contact-line motion: (*a*) General case of mobile contact lines; (*b*) Case of fixed contact angle

or $\dot{A} = 0$ if the angle is ϕ_A or ϕ_R. We see this in the limit $V_A = V_R = \infty$ of (4.8), (4.22) and (4.28). All three expressions give

$$h_0 = (M-\gamma)\exp(-x) \tag{5.4a}$$

or

$$h_0 = -\gamma\exp(-x), \tag{5.4b}$$

which describe static menisci.

Further, we note that when $V_A = V_R = \infty$, (4.11) and (4.25) become

$$\cos t_1 = \cos t_3 = 0, \tag{5.5}$$

so that $t_1 = \frac{1}{2}\pi$ and $t_3 = \frac{3}{2}\pi$. Therefore, the periodic motion of the contact line for the case of fixed angle proceeds as follows: At the top of the plate cycle $\theta = \phi_R$. As the plate is pushed in, the contact line remains fixed to it until θ changes to ϕ_A. Then the contact line advances with speed $(-\cos t)$ until $t = \frac{3}{2}\pi$ and the plate is at the bottom of the cycle. Then the plate is pulled out and the contact line remains fixed until θ changes to ϕ_R. Here the contact line recedes with speed $(-\cos t)$ until $t = \frac{5}{2}\pi$ and the plate is at the top of the cycle. This motion is then repeated, see table 2.

There is, however, one defect in the above description. We must have (5.1) satisfied during the fixed-line portion of the motion and (5.3) satisfied during the fixed-angle portions. $\dot{A}_0$ equals $\cos t$ for the former, yet $\dot{A}_0 \equiv 0$ for the latter. Since the transition between them occurs at t_2 and t_4 we shall necessarily have a *jump in the speed of the contact line* at these times, unless

$$\cos t_2 = \cos t_4 = 0; \tag{5.6}$$

see figure 5. However, we clearly see from (4.17) and (4.26) that $t_2 \neq \frac{1}{2}\pi$ and $t_4 \neq \frac{3}{2}\pi$ unless

$$M = 0, \tag{5.7}$$

and $t_2 \neq \frac{3}{2}$, $t_4 \neq \frac{5}{2}$ unless

$$M = 2. \tag{5.8}$$

The first statement (5.7) would imply no hysteresis, while the second (5.8) would imply that the contact lines remain fixed throughout the plate cycle. This happens

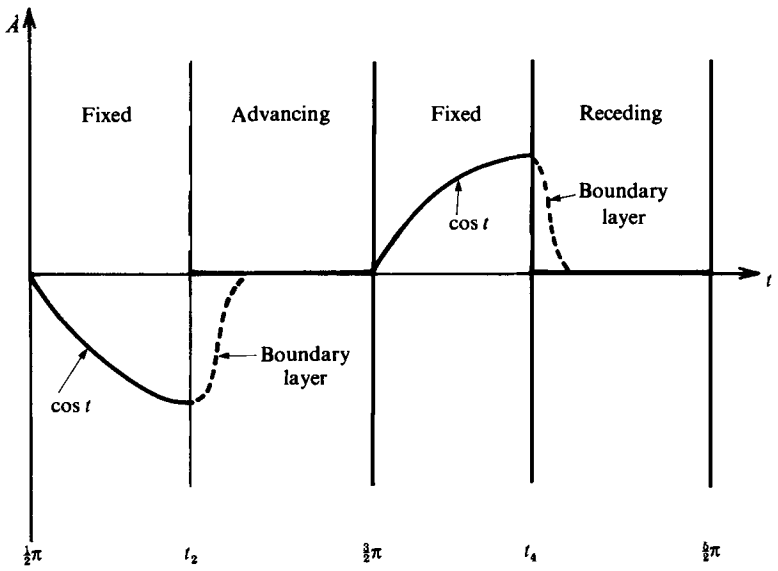

FIGURE 5. Sketch of the (laboratory frame) contact-line speed for the case of fixed contact angle. Boundary-layer corrections in time are present when the fixed contact-angle assumption is relaxed.

because the hysteresis is so large and the plate cycle amplitude so small, that the contact angle cannot change from ϕ_R to ϕ_A during a complete stroke of the plate.

This jump in the contact-line speed can be explained after an examination of the contact-line boundary condition (2.14). If $V_A = V_R = \infty$ in this expression, then we lose the $\dot{A}$-term on the right-hand side. Therefore, this limit of fixed contact angle is a singular perturbation of (2.14). If one applies the method of matched asymptotic expansions, boundary-layer corrections near t_2 and t_4 can be found; see the dotted-line portions of figure 5. These corrections are nothing more than the time-exponential terms in (4.8), (4.22) and (4.28).

Since the $\theta = G(U_{CL})$ curve represents a material characteristic, our results indicate that no materials may exhibit the *exact* fixed contact-angle form, but rather they may only approach it.

We now consider general values of V_A and V_R and allow both γ and M to vary. For all cases we plot the position of the contact line relative to the interface height as $x \to \infty$. The point h_p marked on the plate is at $y = 1$ at the top of the cycle, $t = \frac{1}{2}\pi$, and $y = -1$ at the bottom, $t = \frac{3}{2}\pi$. In addition, we plot the actual contact-line speed, and the laboratory contact-line speed.

In figures 6–8 we consider a symmetric angle-speed characteristic and set $V_A = V_R = V$. We see that for $V = 75$, the response is near that described for fixed contact angles, while for $V < 0.05$, the response is near that for fixed contact lines. Figure 6 shows that the contact lines move more in the laboratory as V gets smaller. This is because the contact lines are becoming less mobile and slip less relative to the plate. Note too the development of the contact-line-speed boundary layer in figure 8 as V gets large.

Table 3 lists the transition times t_1–t_4 for this case. From the differences listed and the figures we see that the response is symmetric whether the contact line is advancing or receding, a consequence of $V_A = V_R$. Figures 9–11 show that this symmetry is not present when $V_A \neq V_R$. From the results for $V_A = 75$, $V_R = 3$ and

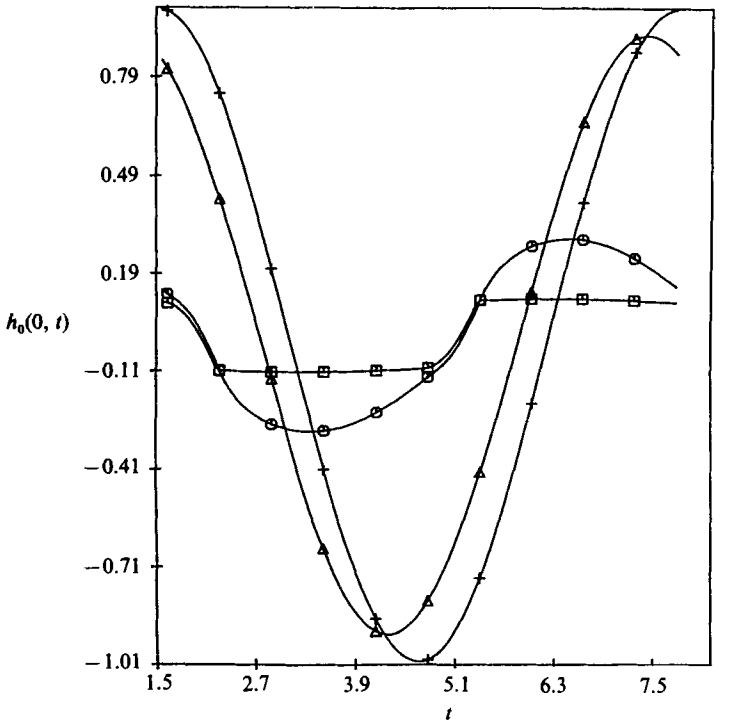

FIGURE 6. The interface position at the contact line versus time for the case $G'(0^+) = G'(0^-)$. ⊡, $V = 75.0$; ⊙, 5.0; △, 0.50, +, 0.05. $\gamma = 0.1$, $M = 0.2$.

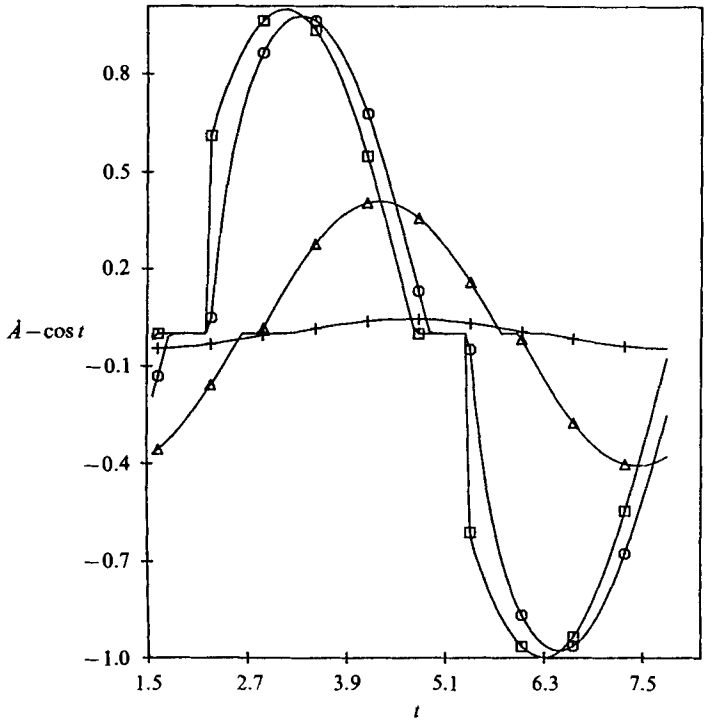

FIGURE 7. The contact-line speed versus time for the case $G'(0^+) = G'(0^-)$. $\gamma = 0.1$, $M = 0.2$. Symbols as figure 6.

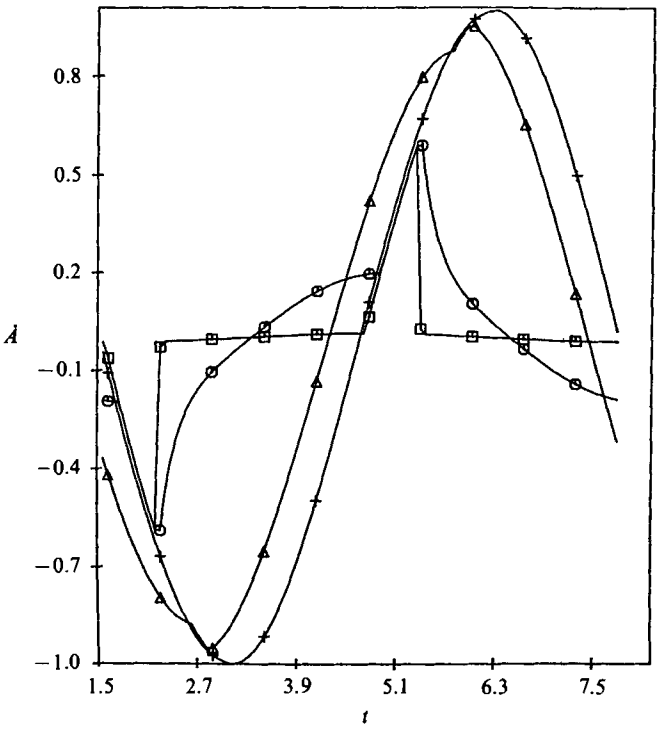

FIGURE 8. The (laboratory frame) contact-line speed versus time for the case $G'(0^+) = G'(0^-)$. $\gamma = 0.1$, $M = 0.2$. Symbols as figure 6.

Type	$\frac{1}{2}\pi$	t_1	t_2	t_2-t_1	t_3	t_4	t_4-t_3	$\frac{5}{2}\pi$	U_{CL} at $t=\frac{1}{2}\pi$
$V_A = 75.0$ $V_R = 75.0$	1.5708	1.5841	2.2144	0.6303	4.7257	5.3560	0.6303	7.8540	−0.0133
$V_A = 5.0$ $V_R = 5.0$	1.5708	1.7682	2.2460	0.4778	4.9098	5.3876	0.4778	7.8540	−0.1923
$V_A = 0.5$ $V_R = 0.5$	1.5708	2.6374	2.8546	0.2172	5.7788	5.9960	0.2172	7.8540	−0.3690
$V_A = 0.05$ $V_R = 0.05$	1.5708	2.9963	3.1968	0.2005	6.1425	6.3430	0.2005	7.8540	−0.0448
$V_A = 5.0$ $V_R = 3.0$	1.5708	1.8926	2.2955	0.4029	4.9098	5.3876	0.4778	7.8540	−0.3000
$V_A = 3.0$ $V_R = 5.0$	1.5708	1.7680	2.2460	0.4780	5.0341	5.4371	0.4030	7.8540	−0.1919

TABLE 3. For the given values of the advancing and receding contact-line speed ratios V_A and V_R, the transition times t_1 to t_4 are shown. At the top of the plate cycle, $t = \frac{1}{2}\pi$, the contact-line speed is negative so the plate is receding. At $t = t_1$, the contact-line speed is zero and the contact angle is ϕ_R. At $t = t_2$, the contact-line speed is zero and the contact angle is ϕ_A. During (t_1, t_2) the contact line remains fixed. During (t_2, t_3) the contact line advances. At $t = t_3$, the contact-line speed is zero and the contact angle is ϕ_A. At $t = t_4$, the contact-line speed is zero and the contact angle is ϕ_R. During (t_3, t_4) the contact line is fixed. From $t = t_4$ through $t = \frac{5}{2}\pi$, when the plate is at the top of the cycle again, the contact line recedes. The quantities t_2-t_1 and t_4-t_3 measure the amount of time the contact line is fixed

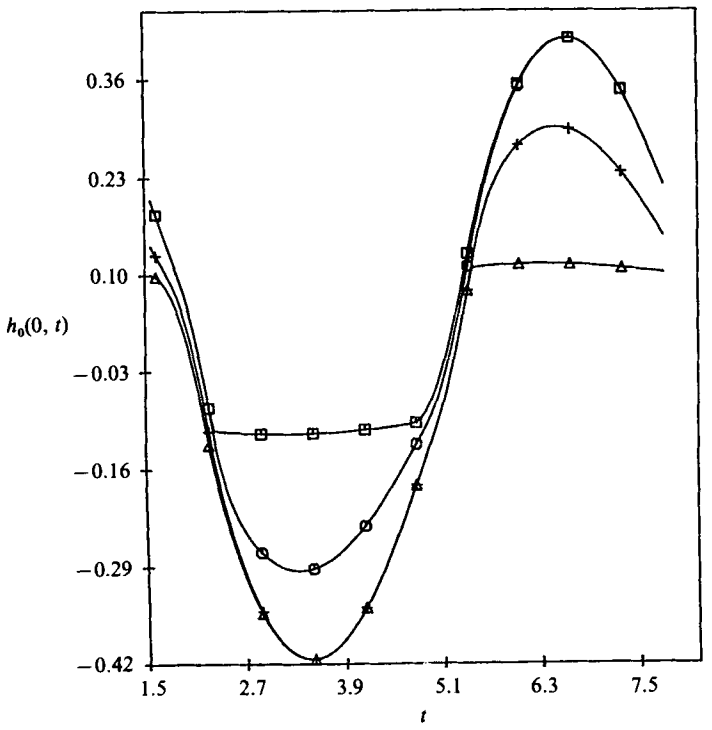

FIGURE 9. The interface position at the contact line versus time for the case $G'(0^+) \neq G'(0^-)$. ⊡, $V_A = 75.0$ and $V_R = 3.0$; ⊙, $V_A = 5.0$ and $V_R = 3.0$; △, $V_A = 3.0$ and $V_R = 75.0$; +, $V_A = 3.0$ and $V_R = 5.0$. $\gamma = 0.1$, $M = 0.2$.

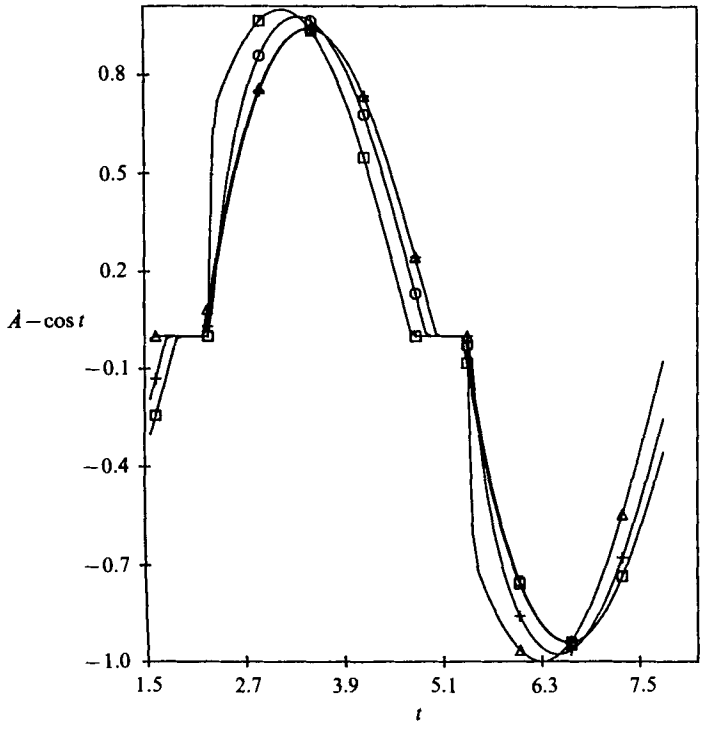

FIGURE 10. The contact-line speed versus time for the case $G'(0^+) \neq G'(0^-)$. $\gamma = 0.1$, $M = 0.2$ Symbols as figure 9.

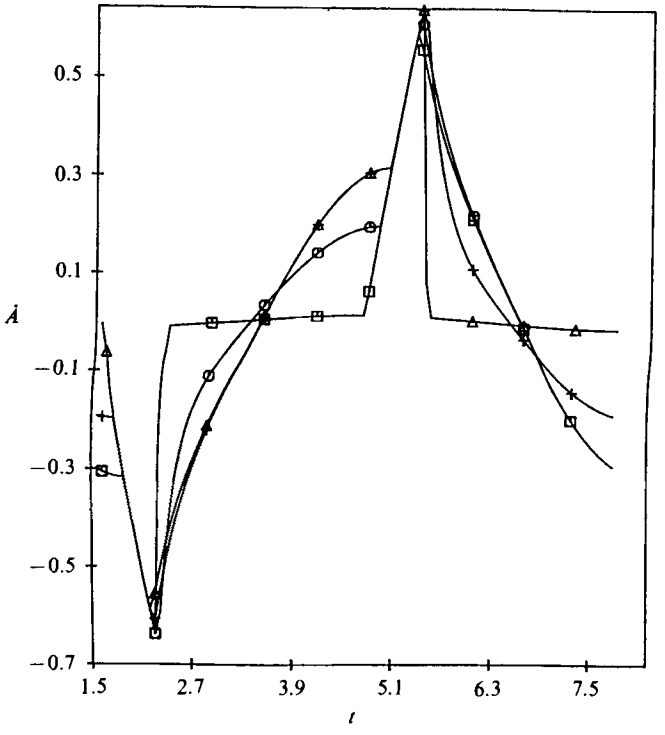

FIGURE 11. The (laboratory frame) contact-line speed versus time for the case $G'(0^+) \neq G'(0^-)$. $\gamma = 0.1$, $M = 0.2$. Symbols as figure 9.

$V_A = 5$, $V_R = 3$ we see that the contact lines advance differently yet recede similarly. Thus the advancing and receding motions differ.

Note from table 3 that the transition times $(t_2 - t_1)$, and $(t_4 - t_3)$ between the advancing and receding motions decrease as V decreases. This appears to be counterintuitive since decreasing V implies that the contact lines are becoming less mobile. Thus, one might expect them to behave for longer as fixed contact lines. Yet our results imply that the amount of time when they are fixed is smaller than for the fixed contact-angle case. This can be explained by considering (4.17) and (4.26) which define t_2 and t_4. As noted before, these depend upon the plate motion through $\sin t_1$ and $\sin t_3$, together with the $\sin^{-1}$ expression. Table 3 shows that $t_1 \to \pi$ and $t_3 \to 2\pi$ as V decreases. The plate speed, $V_p = \cos t$, is a maximum at these two times. Therefore, the transition occurs earlier because the plate is moving faster.

Figures 12–14 show the results for varying M while keeping the other parameters fixed. In figure 13 the zero-speed portions occur over a longer length of time for large M. Note that for $M = 0$, the case of zero hysteresis, there are no fixed portions. The advancing and receding angles, ϕ_A and ϕ_R, are equal for this case so that the transition between the advancing and receding motion occurs instantaneously. Figure 12 shows wide variations in the amount of interfacial motion that occurs. The higher-hysteresis systems tend to deform most. The majority of this deformation takes place when the contact lines are fixed. Figures 13 and 14 show that the contact-line speeds vary only during this time. Thus, the response of the contact line is extremely sensitive to the amount of hysteresis in the system.

Finally, we vary γ keeping all other parameters fixed. Figures 15–17 show that γ only affects the position of the contact line and not the speed. This supports the idea that the contact-line speed depends upon the deviation of the dynamic contact angle

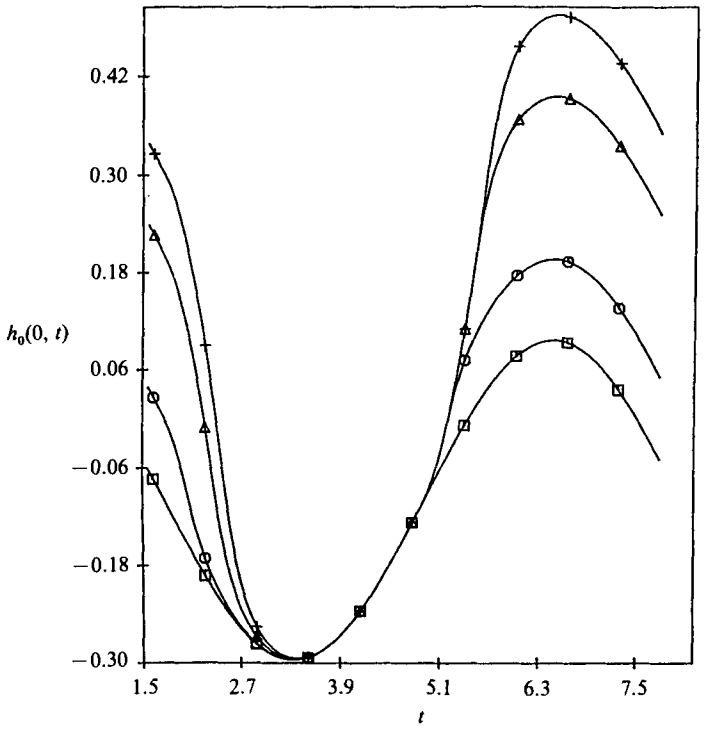

FIGURE 12. The interface position at the contact line versus time for the case $G'(0^+) = G'(0^-)$. $\gamma = 0.1$ and $V_A = V_R = 5.0$. ⊡, $M = 0$; ⊙, 0.1; △, 0.3; +, 0.4.

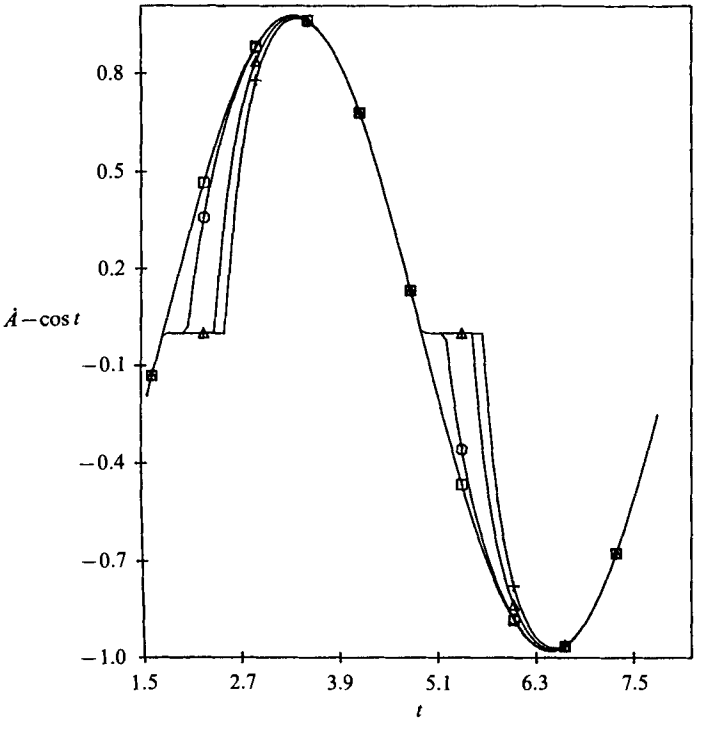

FIGURE 13. The contact-line speed versus time for the case $G'(0^+) = G'(0^-)$. $\gamma = 0.1$ and $V_A = V_R = 5.0$. Symbols as figure 12.

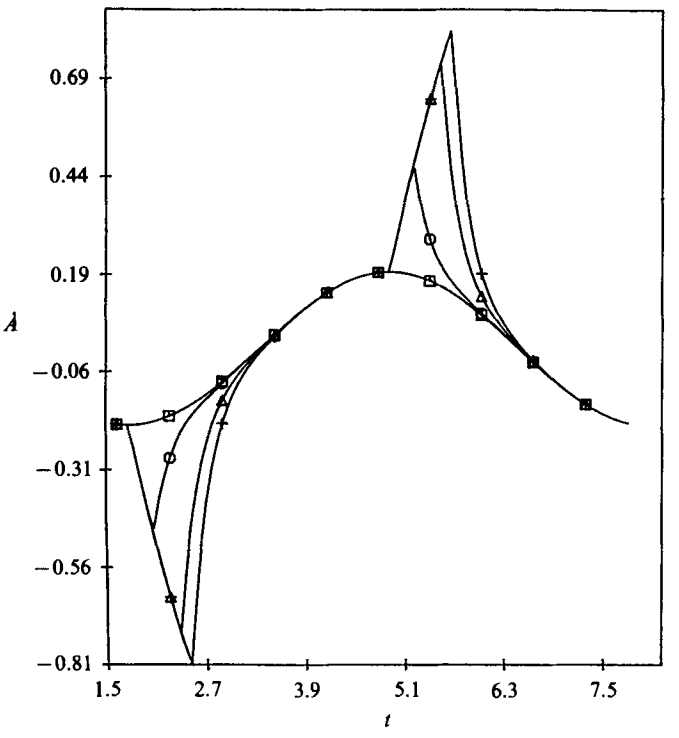

FIGURE 14. The (laboratory frame) contact-line speed versus time for the case $G'(0^+) = G'(0^-)$. $\gamma = 0.1$ and $V_A = V_R = 5.0$. Symbols as figure 12.

from the equilibrium values ϕ_A and ϕ_R, and not on ϕ_A and ϕ_R themselves. We see from figure 15 that varying γ just translates the position of the interface as all four curves can be superposed. As γ decreases and becomes negative, ϕ_A assumes a value smaller than $\frac{1}{2}\pi$. Princen (1969) gives the following expression for the static position of the contact line of a fluid against a motionless flat vertical wall:

$$h_{CL} = 2L_c \sin(\tfrac{1}{4}\pi - \tfrac{1}{2}\theta). \tag{5.9}$$

This expression predicts that h_{CL} increases as θ decreases from $\frac{1}{2}\pi$, consistent with our figure 15. Murphy (1984) used (5.9) as the starting point for her analysis. However, in the limits $\alpha \to 0$, and $C \to 0$, her approach and the approach used here are equivalent.

Figures 18, 19, 20 and 21 give plots of $\hat{F}$ versus the scaled depth of plate immersion.

$$\hat{H} = 1 - \sin t, \tag{5.10}$$

which is obtained from (3.1) by neglecting that portion of the plate still submerged at the top of the stroke. In figure 18, $V_A = V_R = V$, and $M = 0.2$. Note that the openness of the curves represents a dissipation of energy in the system. The magnitude of $\hat{F}$ appears to increase as the contact lines become less mobile, as measured by decreasing V. Thus, a larger suspension force F is required to oscillate the plate when the contact lines are nearly fixed.

Figure 19 in which $V_A \neq V_R$ shows asymmetrical motion compared with figure 18 where $V_A = V_R$.

In figure 20 we vary the amount of hysteresis M in the system while keeping all other parameters fixed. Here $V_A = V_R \neq 0$ so that the contact lines are mobile and the contact angle steepens as the contact-line speed increases. We see that the curves

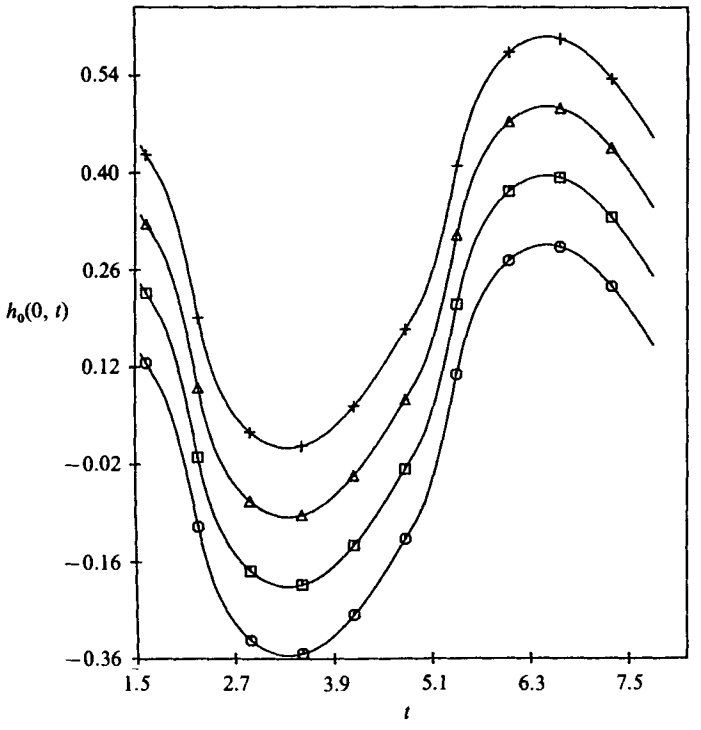

FIGURE 15. The interface position at the contact line versus time for the case $G'(0^+) = G'(0^-)$, $M = 0.2$ and $V_A = V_R = 5.0$. ⊡, $\gamma = 0$; ⊙, $\gamma = 0.1$; △, $\gamma = -0.1$; +, $\gamma = -0.2$. $\gamma > 0$ means $\phi_A = \frac{1}{2}\pi$.

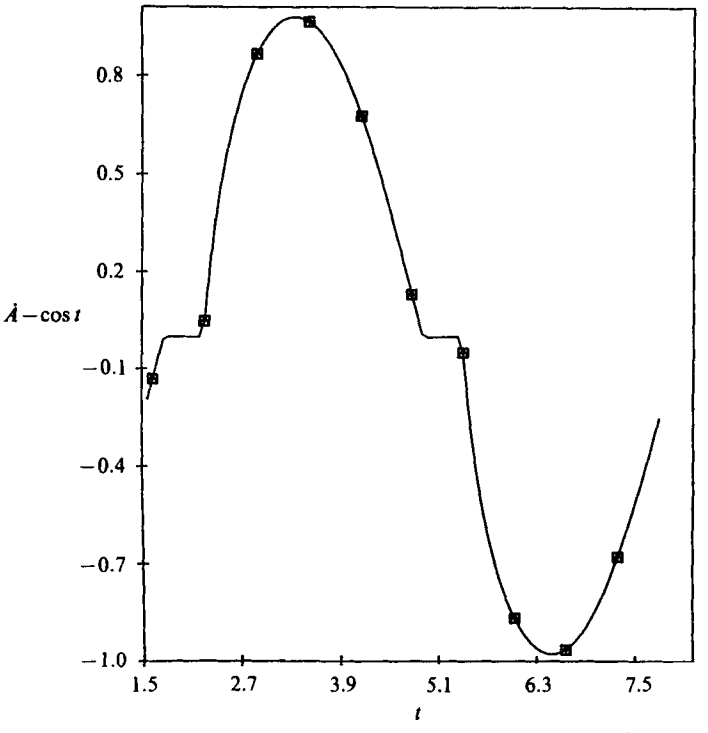

FIGURE 16. The contact-line speed versus time for the case $G'(0^+) = G'(0^-)$, $M = 0.2$ and $V_A = V_R = 5.0$. $\gamma > 0$ means $\phi_A = \frac{1}{2}\pi$. Symbols as figure 15. All curves appear to coincide.

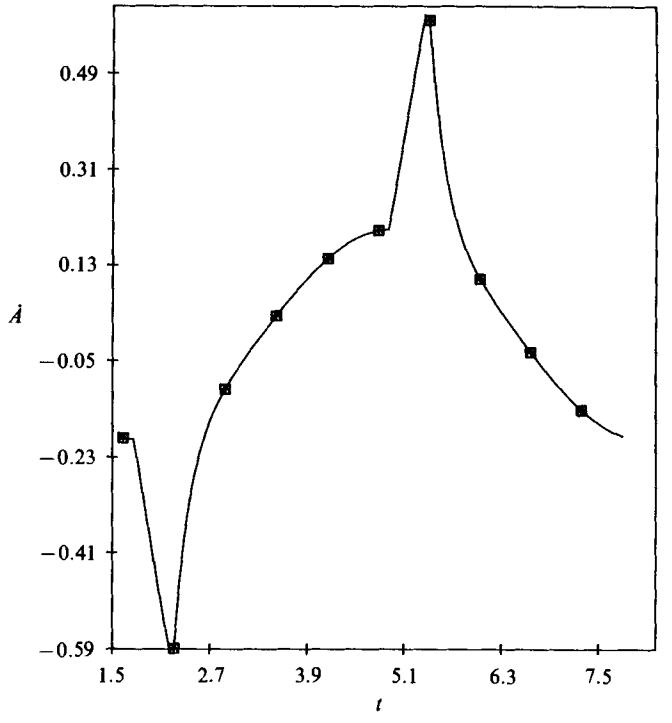

FIGURE 17. The (laboratory frame) contact-line speed versus time for the case $G'(0^+) = G'(0^-)$, $M = 0.2$ and $V_A = V_R = 5.0$. $\gamma > 0$ means $\phi_A = \frac{1}{2}\pi$. Symbols as figure 15. All curves appear to coincide.

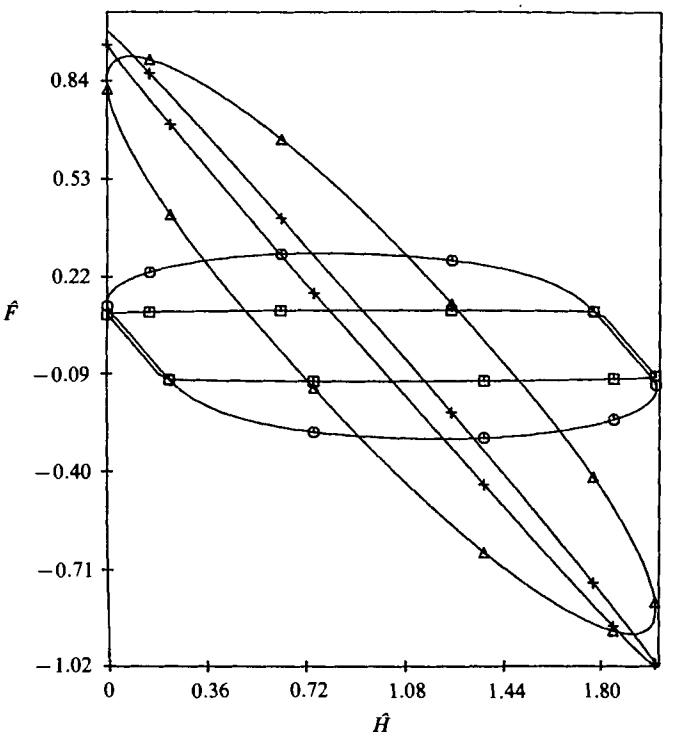

FIGURE 18. The force versus the depth of immersion of a cycle for the case $G'(0^+) = G'(0^-)$. ⊡, $V = 75.0$; ⊙, 5.0; △, 0.50; +, 0.05. $\gamma = 0.1$, $M = 0.2$.

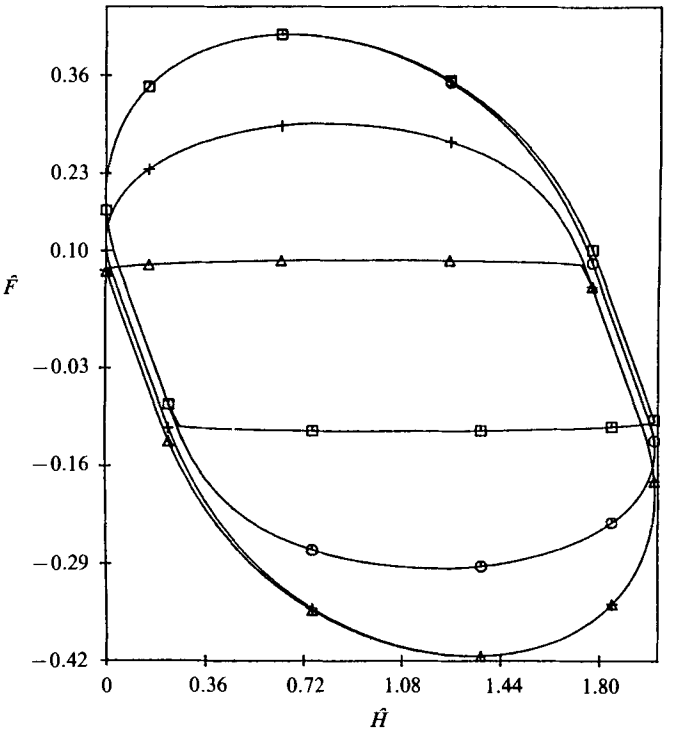

FIGURE 19. The force versus the depth of immersion for cycle for the case $G'(0^+) \neq G'(0^-)$. ⊡, $V_A = 75.0$ and $V_R = 3.0$; ⊙, $V_A = 5.0$ and $V_R = 3.0$; △, $V_A = 3.0$ and $V_R = 75.0$; +, $V_A = 3.0$ and $V_R = 5.0$. $\gamma = 0.1$, $M = 0.2$.

in figure 20 are open, even for $M = 0$, and that the degree of openness increases as M increases. This suggests that contact-angle hysteresis has a dissipative effect on a fluid/fluid/solid system and this effect increases for larger hysteresis. Furthermore, since the curves are also open when there is no hysteresis, then aspects of the mobility of the contact lines also represent a dissipative process. Thus, the openness of the curves of figures 18, 19 and 20 is due to dissipative contributions from the presence of contact-angle hysteresis *and* increase of the contact angle with contact-line speed.

In figure 21 all parameters are held fixed except the deviation of the advancing contact angle ϕ_A from $\frac{1}{2}\pi$. When $\gamma < 0$ the interface near the contact line is concave up and surface-tension forces tend to pull the plate into the fluid. Thus, a larger suspension force F is needed. On the other hand, when $\gamma > 0$, the interface is concave down and surface-tension forces tend to pull the plate out of the fluid. Here, a smaller suspension force is required.

In summary, our force versus depth-of-immersion curves further support the notion that the increase of the contact angle with contact-line speed is a dissipative process as suggested by Davis (1980). The strength of this contribution to the overall dissipation in the system appears to go to zero as $G'(0)$ approaches zero and infinity. In figure 22, for $M = 0$, we plot the immersion curves for varying V, i.e. for varying $G'(0)$. Note that the openness of the curves approaches zero as $V \to 0$ and ∞, the fixed-contact-line and fixed-contact-angle limits.

In addition we find that the greater the contact-angle hysteresis present in the system, the greater is the openness of the immersion curve. However, in lieu of the

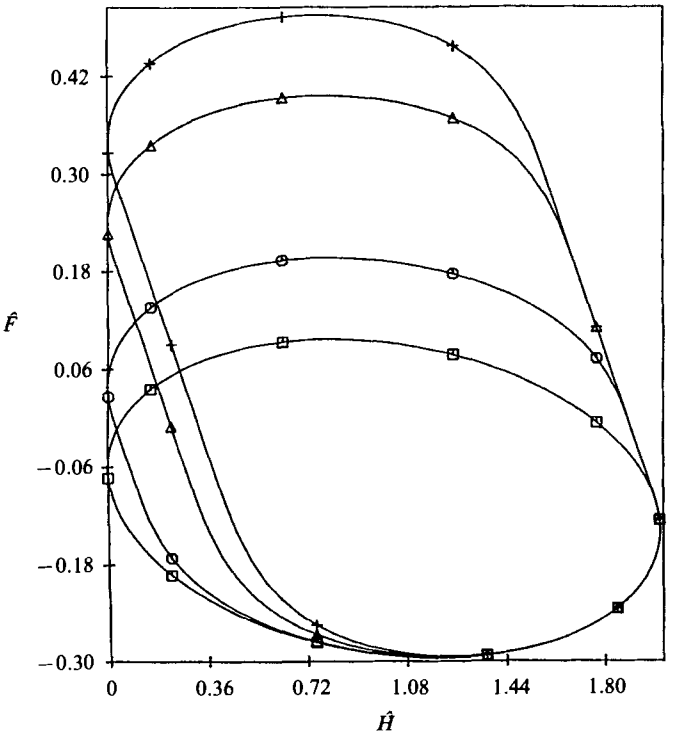

FIGURE 20. The force versus depth of immersion for a cycle for the case $G'(0^+) = G'(0^-)$. $\gamma = 0.1$ and $V_A = V_R = 5.0$. ⊡, $M = 0$; ⊙, 0.1; △, 0.3; +, 0.4.

fixed-contact-line result shown in figure 22, the latter statement appears to be true only when the hysteresis $M\alpha$ is small. When $M\alpha$ is large compared to the amplitude of the plate motion, the contact line is fixed to the plate throughout the motion. Hence, there is no dissipation. Thus, contact-angle hysteresis appears to also contribute to the dissipation in the system. This effect increases the dissipation as the hysteresis increases from zero but becomes negligible as the magnitude of the hysteresis becomes large. This suggests that contact-angle hysteresis may act as a stabilizing mechanism to contact-line disturbances. Such a conjecture was also proposed by Weiland & Davis (1981), although for different reasons.

6. Square-wave plate motion

There is a related analysis by Murphy (1984) of a square-wave plate motion as shown in figure 23. This analysis uses a somewhat different approach yet it is instructive to cast her results into our notation and to pose it in terms of our approximations.

In that work the plate speed is assumed to be a constant so that the $\cos t$ term in (2.14) is replaced by the scaled constant speed of the plate. This motion is an idealization of the constant-speed-plate motion that experimenters approach using the Wilhelmy plates (Penn & Miller 1980*a*, *b*; Johnson, Dettre & Brandreth 1977).

Suppose that the plate speed has the constant value $2D\omega/\pi$, so that the maximum depth of the plate immersion is $2D$. In this case we replace the $\cos t$ term in (2.14)

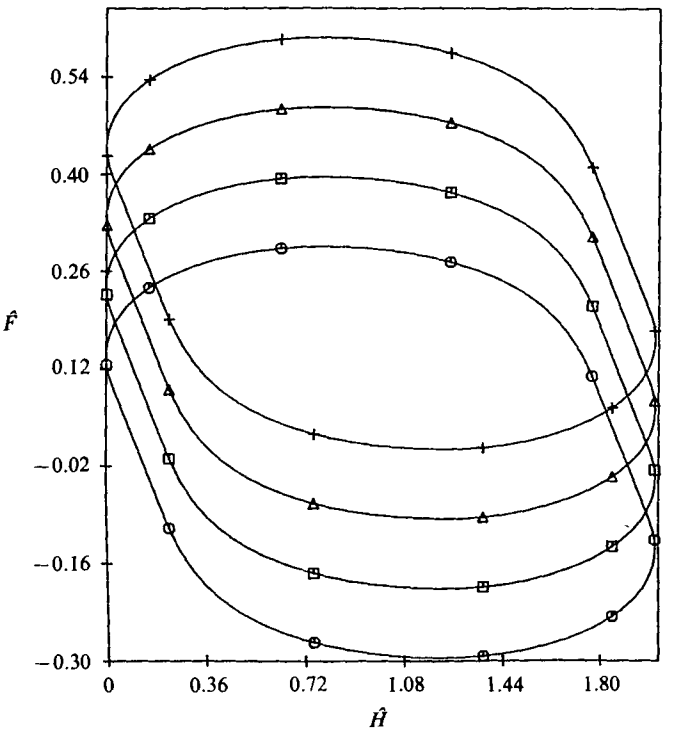

FIGURE 21. The force versus the depth of immersion for a complete cycle for the case $G'(0^+) = G'(0^-)$, $M = 0.2$ and $V_A = V_R = 5.0$. ⊡, $\gamma = 0$; ⊙, 0.1; △, −0.1; +, −0.2. $\gamma > 0$ means $\phi_A = \frac{1}{2}\pi$.

by $\pm 2/\pi$, depending upon whether the plate is withdrawn from or pushed into the liquid. As before, we calculate the contact-line position and speed. For instance,

$$U_{CL} = \dot{A}_0 + \frac{2}{\pi} \tag{6.1}$$

when the plate is pushed in and the contact line is advancing. Here $\dot{A}_0$ has the form

$$\dot{A}_0 = -V_A C_0^+ \exp(-V_A t) \tag{6.2}$$

and we have an analogous expression during the receding motion. The corresponding contact angle for the advancing motion is related to

$$h_{0x} = -C_0^+ \exp(-V_A t) + \gamma + \frac{2}{\pi V_A}. \tag{6.3}$$

Both (6.2) and (6.3) show that for large values of t the speed of the contact line and the contact angle tend toward steady-state values. In particular the velocity of the contact line approaches the negative of the plate velocity, while the contact angle takes on a dynamic value greater than ϕ_A. In the case of a receding motion, we find that the dynamic contact angle takes on a value less than ϕ_R.

In figure 24 we plot a family of immersion curves for a fixed value of $D\omega$ corresponding to

$$\frac{V_A}{\alpha} = \frac{V_R}{\alpha} = \frac{1}{D\omega G'(0)} = 1000. \tag{6.4}$$

Here $\gamma\alpha = \pi/36$ and $M\alpha = \pi/18$. Such values describe either a material system with very mobile contact lines, $G'(0)$ small, or one run at a low plate speed. Note that

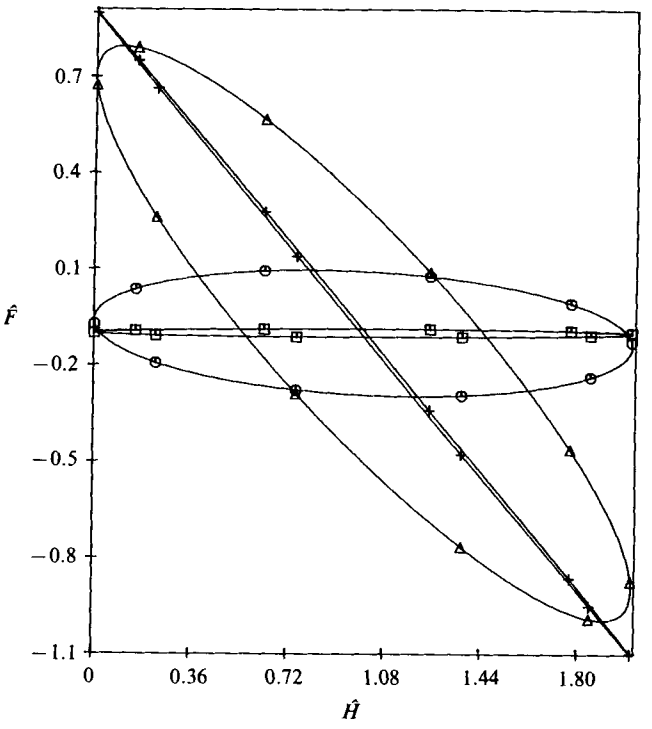

FIGURE 22. The force versus the depth of immersion for a cycle for the case $G'(0^+) = G'(0^-)$, $M = 0$ and $\gamma = 0.1$. ⊡, $V = 80.0$; ⊙, 5.0; △, 0.50; +, 0.01.

increasing α corresponds to increasing D so that the plate is plunged further into the bath at lower frequencies. The upper and lower horizontal asymptotes give $\cos\phi_R$ and $\cos\phi_A$ respectively, to within 0.01 %. However, one can make no conclusions regarding the value of $G'(0)$ at this point. It could either be small, implying that we are dealing with a material system described by a nearly fixed contact-angle behaviour, or we could be at such a low plate speed, $2D\omega/\pi$, that the contact angles have time to adjust to the equilibrium values.

Now consider figure 25, where $V_A/\alpha = V_R/\alpha = 10$. If we are dealing with the same material system as in figure 24, this is realized by increasing the plate speed $2D\omega/\pi$. For α as in figure 24 this can be done by running the plate at a higher frequency ω. For $\alpha > 0.796$, the curves again exhibit upper and lower horizontal asymptotes corresponding to the minimum and maximum angles encountered in the plate cycle. Here for instance, the maximum advancing contact angle is 5.7° larger than ϕ_A. This is to be expected since the contact angle tends to increase with increasing contact-line speed as induced by the increasing speed of the plate.

However, we see for $\alpha < 0.796$ that a horizontal asymptote does not exist. In these cases the frequency of plate motion is so large compared with the amplitude $2D$, as measured by α, that the contact-line velocity never attains the steady-state value equal in magnitude to the plate speed but oppositely directed. In other words, for this ω the plate does not plunge far enough into the bath for the contact line to reach the steady-state value. This situation can be remedied by either increasing the plate stroke $2D$ or decreasing the plate frequency ω.

These results suggest a method for determining ϕ_A, ϕ_R, $G'(0^+)$ and $G'(0^-)$ from measurements of the force on a moving plate as a function of its depth of immersion.

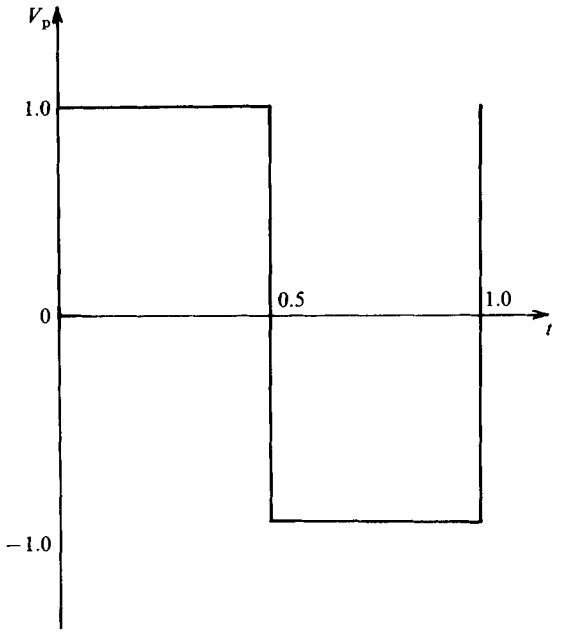

FIGURE 23. The plate speed V_p versus t for one cycle.

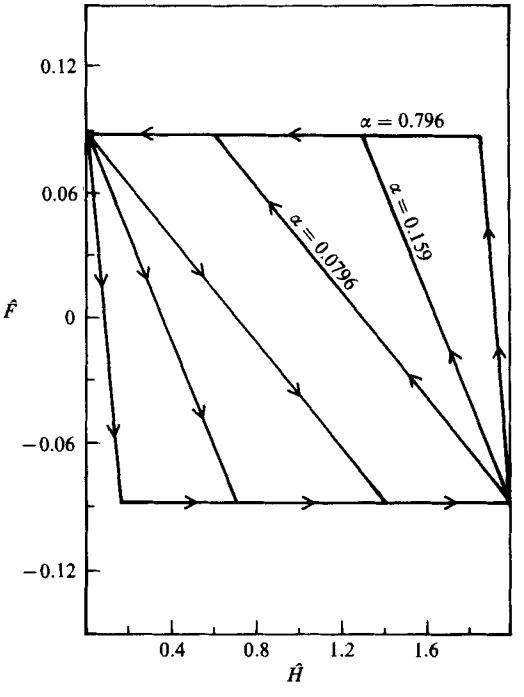

FIGURE 24. The force versus the depth for the square-wave motion for the case $V_A/\alpha = V_R/\alpha = 1000$, $\gamma\alpha = \pi/36$ and $M\alpha = \pi/18$.

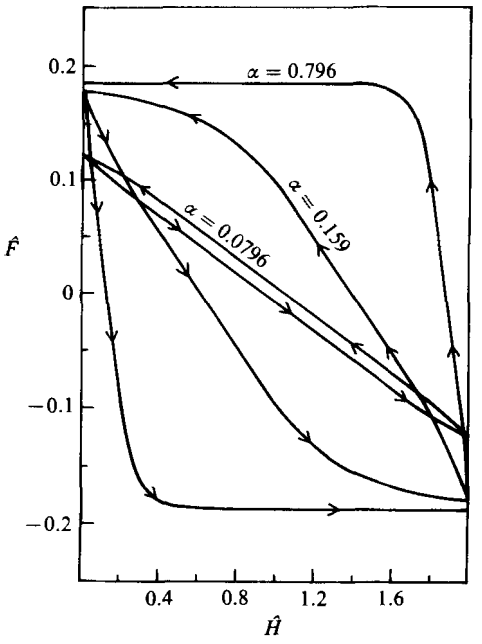

FIGURE 25. The force versus the depth for the square-wave motion for the case $V_A/\alpha = V_R/\alpha = 10$, $\gamma\alpha = \pi/36$ and $M\alpha = \pi/18$.

First, measure the dimensional force and depth of immersion for a square-wave forcing function with a particular maximum plate speed $2D\omega/\pi$. In making these measurements, we must ensure that the frequency of motion of the plate ω is sufficiently small that the contact-line speed attains its steady-state value $U_{CL} = -2D\omega/\pi$.

Once the dimensional F and H data have been taken, $\hat{F}$ can be calculated using (3.4*b*) modified for zero acceleration of the plate and a linear law for the depth of immersion. $\hat{F}$ may then be plotted as a function of $\hat{H} = H/D$. The upper asymptote of the resulting immersion curve gives the cosine of the dynamic contact angle at $U_{CL} = -2D\omega/\pi$. The lower asymptote gives the dynamic contact angle at $U_{CL} = 2D\omega/\pi$. If upper and lower asymptotes do not exist, the experiment should be repeated at a smaller ω.

This process can now be repeated for different $D\omega$ values. In this way, the dependence of θ on U_{CL} can be measured. For U_{CL} greater than zero, the slope of the curve gives $G'(0^+)$, and the y-intercept gives ϕ_A. Similarly, for U_{CL} less than zero, the slope gives $G'(0^-)$ and the intercept ϕ_R.

It should be emphasized that our analysis is valid only for small values of α, for small C, and for a linear relationship between θ and U_{CL}. Murphy (1984) claims validity of her analysis at larger α. By running the experiments at the smallest practical $D\omega$-values, we achieve the smallest α-value and guarantee that C is also small. The assumption of a piecewise-linear relationship between θ and U_{CL} is a convenience, more general forms are easily incorporated.

7. Conclusions

We have considered the oscillatory motion of a solid plate into and out of a bath of liquid. The problem is taken to be two-dimensional so that the contact line is straight, and can be viewed as an advancing or receding front of liquid.

In order to study the effects of hysteresis for a continuous motion of the plate, we take the plate displacement to be sinusoidal with non-dimensional amplitude α and period 2π. For small capillary number C we consider that the static advancing contact angle ϕ_A is $\phi_A = \frac{1}{2}\pi + \gamma\alpha$ and that the contact-angle hysteresis is $\phi_A - \phi_R = M\alpha$, where γ and M are $O(1)$ as $\alpha \to 0$. Further we take the characteristic of contact angle versus contact-line speed to be piecewise linear, with $G'(0^+)$ and $G'(0^-)$ measuring the slopes for advancing and receding portions respectively.

Our analysis shows that the contact-line mobilities enter through the numbers V_A and V_R, viz.

$$V_A = \frac{1}{L_c \omega G'(0^+)}, \quad V_R = \frac{1}{L_c \omega G'(0^-)}, \tag{7.1}$$

where ω is the angular frequency of oscillation of the plate and L_c is the capillary length $(\sigma/\rho g)^{\frac{1}{2}}$.

For small α, $\alpha = D/L_c$, where $2D$ is the displacement amplitude of the plate, we obtain 2π-periodic contact-line motions that develop after initial transients have decayed.

We find that the contact line moves with the plate if the contact line is fixed but has relative motion otherwise. It would then advance part of the time, recede part of the time and remain stationary in the transition periods.

Dependence on γ. The departure of ϕ_A from $\frac{1}{2}\pi$ affects the position of the interface near the contact line. If $\gamma < 0$ so that $\phi_A < \frac{1}{2}\pi$, the contact line tends to climb the plate forming a concave-upward interface. If $\gamma > 0$ so that $\phi > \frac{1}{2}\pi$, the contact line crawls downward forming a concave-downward interface. The value of γ does not affect the speed of the contact line nor the time intervals when the contact line is fixed. The contact-line speed depends on differences between θ from ϕ_A or ϕ_R and not on ϕ_A and ϕ_R individually. Likewise, the hysteresis affects the length of time that the contact-line remained stationary through $\phi_A - \phi_R$ and not on ϕ_A itself.

Dependence on M. The amount of hysteresis in the system directly affects the time intervals during which the contact line is fixed. These times approach zero as M approaches zero, and they increase as M increases. Thus, when hysteresis is present, the contact lines must remain fixed to the plate as the contact-line motion changes from an advancing to a receding state or vice-versa since this transition does not occur instantaneously. The larger the hysteresis in the system, the longer it takes.

Dependence on V_A and V_R. These parameters measure the mobility of the contact line and have the strongest influence on the position of the contact line, the contact-line speed and the contact angle. In light of (7.1), suppose that ω and L_c are fixed and that $G'(0^+) = G'(0^-) \equiv G'(0)$, which implies a symmetric response for the immersion and emersion portions of the cycle.

The limit $G'(0) \to \infty$ implies that the contact line is fixed to the plate. We have shown that $V_A = V_R = 0$ results in the contact line always following the plate with the speed of the contact line relative to the plate being zero. Hysteresis has no effect for this motion.

The limit $G'(0) \to 0$ implies that the contact angle is fixed. We have shown that $V_A = V_R \to \infty$ results in the contact angle being fixed at ϕ_A during the time interval

(t_2, t_3) and being fixed at ϕ_R during the interval (t_4, t^*); see table 2. Here $t_1 = t_0$ and $t^* = t_0 + 2\pi$. At these times the velocity of the contact line is exactly opposite that of the plate so that the contact line looks stationary to an observer. During the interval (t_1, t_2) the contact line is fixed as θ varies from ϕ_R to ϕ_A; during the interval (t_3, t_4) the contact line is fixed as θ varies from ϕ_A to ϕ_R. The contact-line speed is zero at these times so that the contact line appears to an observer to move with the plate. We have shown, though that the contact-line motion described here necessarily involves a jump in the contact-line speed at t_2 and t_4. This leads one to question the fixed-contact-angle assumption often posed in contact-line problems.

For values of $G'(0)$ other than zero and ∞, the contact-line motion fits somewhere between the above regimes; see table 2. The contact-line speeds are continuous for these cases. Let us now fix L_c and $0 < G'(0) < \infty$ and consider the effects of varying ω. Since the contact-line motion becomes most pronounced as $G'(0)$ decreases to zero, the contact-line forces are the strongest for that case. Now, as $\omega \to 0$, the plate speed becomes extremely slow. Thus the plate motion impresses little upon the contact line. V_A and V_R become large; the contact angles have time to adjust to the equilibrium values ϕ_A or ϕ_R and it appears that the contact angles are fixed. On the other hand when ω becomes large, but keeping the capillary number small, the plate is moving quickly. This motion is felt by the contact line and it overwhelms the contact-line forces, $G'(0)$. V_A and V_R approach zero and the contact line stays fixed to the plate.

We now fix $0 < \omega < \infty$, and $0 < G'(0) < \infty$ and consider the effects of varying L_c or surface tension. When surface tension is small, the interface is flexible. It will easily distort and the contact-line forces dominate the contact-line motion. V_A and V_R become large. The contact-line forces have little competition and the contact angles adjust to the equilibrium values. Again it appears as though $G'(0)$ approaches zero. Now if surface tension is large, these forces will dominate the contact-line forces. They cannot overcome the stiff interface so the contact line does not move. It stays fixed to the plate and it appears as if $G'(0)$ approaches ∞.

Additionally, the force required to suspend the plate in the bath plotted versus the depth of immersion of the plate shows, over the complete cycle of the plate motion, that energy is dissipated in the system. The mechanisms responsible for this energy dissipation are the presence of contact-angle hysteresis and the steepening of the contact angle with increasing contact-line speed. The former effect is suppressed as the hysteresis becomes large and the contact line stays fixed over a larger portion of the cycle. The latter effect is suppressed for the cases of fixed contact angle and fixed contact line when the contact angle is independent of the speed of the contact line.

The above gives the small capillary number, small-displacement-amplitude response of the contact line when hysteresis is present and the plate motion is continuous. Most experimentalists aim to use a plate motion in which the plate speed is constant so that one can accurately measure the angle. The same type of analysis used for the sinusoidal motion of the plate has also been applied to a square-wave form for the plate speed. We have obtained force-displacement curves again showing the care that must be taken and the explanation for the loop-area variations seen.

In summary, the major general conclusions of the analysis are as follows:

(1) When hysteresis is present, the contact lines must remain fixed for a non-zero length of time when undergoing a transition from an advancing to a receding motion.

(2) The fixed-contact-angle assumption may lead to physically unrealistic contact-line-speed responses.

(3) Measurements used to determine how the contact angle varies with the speed of the contact line can be misleading owing to dynamical effects in the system. We describe precautions that should be observed to avoid the ambiguity in experiments.

(4) Contact-angle hysteresis and the steepening of the contact angle with increasing contact-line speed are dissipative effects, both of which contribute to the presence of open force-displacement loops.

(5) Even though our results are obtained in the creeping-flow limit, the motion of the contact line tends to lag behind the plate motion in such a way that the contact line still moves although the plate is motionless. Thus, there exists an apparent inertial effect due to contact-line effects.

The authors are grateful to Dr E. B. Dussan V. for valuable discussions and suggestions, particularly on the relationship between our results and the experimental protocols. This work was sponsored by the National Science Foundation, Fluid Mechanics Program.

REFERENCES

DAVIS, S. H. 1980 *J. Fluid Mech.* **98**, 225.

DUSSAN V., E. B. 1979 *Ann. Rev. Fluid Mech.* **11**, 371.

DUSSAN V., E. B. 1985 *J. Fluid Mech.* **151**, 1.

DUSSAN V., E. B. & CHOW, R. T.-P. 1983 *J. Fluid Mech.* **137**, 1.

DUSSAN V., E. B. & DAVIS, S. H. 1974 *J. Fluid Mech.* **65**, 71.

GUASTALLA, J. 1957 In *Proc. Second International Congress of Surface Activity*, III (ed. J. H. Schulman), pp. 143–152. Academic.

JOHNSON, R. E. & DETTRE, R. H. 1969 In *Surface and Colloid Science*, vol. 2 (ed. E. Matijevic), pp. 85–153. Wiley-Interscience.

JOHNSON, R. E., DETTRE, R. H. & BRANDRETH, D. A. 1977 *J. Colloid Interface Sci.* **62**, 205.

MURPHY, E. D. 1984 The moving Wilhelmy plate: a theoretical study. M.S. thesis, University of Pennsylvania, Philadelphia, Pennsylvania.

PENN, L. S. & MILLER, B. 1980*a* *J. Colloid Interface Sci.* **77**, 574.

PENN, L. S. & MILLER, B. 1980*b* *J. Colloid Interface Sci.* **78**, 238.

PRINCEN, H. M. 1969 In *Surface and Colloid Science*, vol. 2 (ed. E. Matijevic), pp. 1–84. Wiley-Interscience.

WEILAND, R. H. & DAVIS, S. H. 1981 *J. Fluid Mech.* **107**, 261.

YOUNG, G. W. 1985 Dynamics and Stability of Flows with Moving Contact Lines. Ph.D. thesis, Northwestern University, Evanston, Illinois.